

## Controlled Electrochemical Synthesis of Conductive Polymer Nanotube Structures

Rui Xiao, Seung Il Cho, Ran Liu, and Sang Bok Lee\*

Contribution from the Department of Chemistry and Biochemistry, University of Maryland, College Park, Maryland 20742

Received December 13, 2006; E-mail: slee@umd.edu

**Abstract:** We have investigated the electrochemical synthetic mechanism of conductive polymer nanotubes in a porous alumina template using poly(3,4-ethylenedioxythiophene) (PEDOT) as a model compound. As a function of monomer concentration and potential, electropolymerization leads either to solid nanowires or to hollow nanotubes, and it is the purpose of these investigations to uncover the detailed mechanism underlying this morphological transition between nanowire and nanotube. Transmission electron microscopy was used to characterize electrochemically synthesized PEDOT nanostructures and measure the extent of their nanotubular portion quantitatively. The study on potential dependency of nanotubular portion shows that nanotubes are grown at a low oxidation potential (1.2 V vs Ag/AgCl) regardless of monomer concentration. This phenomenon is attributed to the predominance of electrochemically active sites on the annular-shape electrode at the pore bottom of a template. The explanation was supported by a further electrochemical study on a flat-top electrode. We elaborate the mechanism by taking into account the effect of electrolyte concentration, temperature, and template pore diameter on PEDOT nanostructures. This mechanism is further employed to control the nanotube dimensions of other conductive polymers such as polypyrrole and poly(3-hexylthiophene).

### Introduction

Nanostructured materials can provide intrinsically high surface area leading to higher charge/discharge capacity and short diffusion distance for ion transport leading to faster charge/discharge rate.<sup>1</sup> Nanotechnologies to synthesize and characterize such nanomaterials are essential to fabricate highly integrated, tiny, and lightweight electronic devices with high performance. Desired nanostructures have been prepared by various methods, such as vapor–liquid–solid process,<sup>2</sup> self-assembly,<sup>3</sup> and template synthesis,<sup>1,4</sup> etc. The template synthesis method has particularly fascinated scientists due to its simplicity and diverse applicabilities. The Martin group has pioneered and extensively studied this method<sup>1,4b,c,5</sup> since it was first reported by Frazier

et al.<sup>6</sup> A variety of materials including metals, conductive polymers, and semiconductors can be deposited within the cylindrical pores of a membrane chemically or electrochemically. The deposition process produces nearly monodispersed nanotubes, nanowires, or nanorods. Furthermore, the dimensions of the deposited nanostructures can be easily controlled by regulating the template pores and deposition conditions.

Conductive polymers are indispensable materials for the development of organic electronic devices, such as electrochemical power sources,<sup>7</sup> flexible electronic devices,<sup>8</sup> and displays.<sup>9</sup> One of the important issues in such electronic devices is the poor charge-transport rate due to slow diffusion of counterions into/out of the conductive polymer during redox processes.<sup>10</sup> Nanotubular structure of conductive polymer is one of the ideal structures that can enhance the device performance by improving charge-transport rate as well as increasing surface

- (1) (a) Van Dyke, L. S.; Martin, C. R. *Langmuir* **1990**, *6*, 1118–1123. (b) Nishizawa, M.; Mukai, K.; Kuwabata, S.; Martin, C. R.; Yoneyama, H. *J. Electrochem. Soc.* **1997**, *144*, 1923–1927. (c) Patrissi, C. J.; Martin, C. R. *J. Electrochem. Soc.* **1999**, *146*, 3176–3180. (d) Li, N.; Martin, C. R.; Scrosati, B. *Electrochem. Solid-State Lett.* **2000**, *3*, 316–318. (e) Yamada, K.; Gasparac, R.; Martin, C. R. *J. Electrochem. Soc.* **2004**, *151*, E14–E19.
- (2) Goldberger, J.; He, R.; Zhang, Y.; Lee, S.; Yan, H.; Choi, H.-J.; Yang, P. *Nature* **2003**, *422*, 599–602.
- (3) Yin, L.-W.; Bando, Y.; Zhan, J.-H.; Li, M.-S.; Golberg, D. *Adv. Mater.* **2005**, *17*, 1972–1977.
- (4) (a) Xia, Y.; Yang, P.; Sun, Y.; Wu, Y.; Mayers, B.; Gates, B.; Yin, Y.; Kim, F.; Yan, H. *Adv. Mater.* **2003**, *15*, 353–389. (b) Martin, C. R. *Science* **1994**, *266*, 1961–1966. (c) Brumlik, C. J.; Martin, C. R. *J. Am. Chem. Soc.* **1991**, *113*, 3174–3175. (d) Johnson, S. A.; Ollivier, P. J.; Mallouk, T. E. *Science* **1999**, *283*, 963–965. (e) Kline, T. R.; Tian, M.; Wang, J.; Sen, A.; Chan, M. W. H.; Mallouk, T. E. *Inorg. Chem.* **2006**, *45*, 7555–7565. (f) Shelimov, K. B.; Moskovits, M. *Chem. Mater.* **2000**, *12*, 250–254.
- (5) (a) Penner, R. M.; Martin, C. R. *J. Electrochem. Soc.* **1986**, *133*, 2206–2207. (b) Klein, J. D.; Herrick, R. D., II; Palmer, D.; Sailor, M. J.; Brumlik, C. J.; Martin, C. R. *Chem. Mater.* **1993**, *5*, 902–904.

- (6) Frazier, S. E.; Bedford, J. A.; Hower, J.; Kenney, M. E. *Inorg. Chem.* **1967**, *6*, 1693–1696.
- (7) (a) Song, H.-K.; Palmore, G. T. R. *Adv. Mater.* **2006**, *18*, 1764–1768. (b) Wang, J.; Yang, J.; Xie, J.; Xu, N. *Adv. Mater.* **2002**, *14*, 963–965.
- (8) (a) Facchetti, A.; Yoon, M.-H.; Marks, T. J. *Adv. Mater.* **2005**, *17*, 1705–1725. (b) Sirringhaus, H.; Kawase, T.; Friend, R. H.; Shimoda, T.; Inbasekaran, M.; Wu, W.; Woo, E. P. *Science* **2000**, *290*, 2123–2126.
- (9) (a) Gaupp, C. L.; Welsh, D. M.; Rauh, R. D.; Reynolds, J. R. *Chem. Mater.* **2002**, *14*, 3964–3970. (b) Argun, A. A.; Aubert, P.-H.; Thompson, B. C.; Schwendeman, I.; Gaupp, C. L.; Hwang, J.; Pinto, N. J.; Tanner, D. B.; MacDiarmid, A. G.; Reynolds, J. R. *Chem. Mater.* **2004**, *16*, 4401–4412. (c) Heuer, H. W.; Wehrmann, R.; Kirchmeyer, S. *Adv. Funct. Mater.* **2002**, *12*, 89–94. (d) Andersson, P.; Nilsson, D.; Svensson, P.-O.; Chen, M.; Malmstrom, A.; Remonen, T.; Kugler, T.; Berggren, M. *Adv. Mater.* **2002**, *14*, 1460–1464.
- (10) (a) Cho, S. I.; Kwon, W. J.; Choi, S.-J.; Kim, P.; Park, S.-A.; Kim, J.; Son, S. J.; Xiao, R.; Kim, S.-H.; Lee, S. B. *Adv. Mater.* **2005**, *17*, 171–175. (b) Cho, S. I.; Choi, D. H.; Kim, S.-H.; Lee, S. B. *Chem. Mater.* **2005**, *17*, 4564–4566.

area. Recently, we have pioneered the electrochemical synthesis of poly(3,4-ethylenedioxythiophene) (PEDOT) nanotubes and their applications in the development of fast electrochromic devices (<40 ms in electrochromic color-change speed).<sup>10</sup> The thin-walled nanotubular structure enables ions to easily diffuse into/out of the conductive polymer, which results in ultrafast color switching rate. However, detailed mechanism studies on the electrochemical synthesis of conductive polymer nanotubes<sup>11</sup> are very limited, despite the importance and high applicability of conductive polymer nanotubes in various electronic devices. It is a challenging problem to understand the electrochemical synthetic mechanism and control the dimensions of the conductive polymer nanotubes.

The synthesis of conductive polymer nanotubes has been performed chemically or electrochemically using various templates.<sup>4b,12</sup> Martin and co-workers pioneered the synthesis of conductive polymer nanotubes and nanofibers such as polypyrroles, polythiophenes, and polyanilines in the pores of a polycarbonate or alumina membrane.<sup>4b,12d,13</sup> The Wan group introduced surfactants as a template as well as dopants to synthesize polyaniline and polypyrrole nanotubes.<sup>14</sup> Nanofibers of biodegradable polymer can be an alternative choice as a template: the conductive polymer is electrodeposited on the surface of electrospun nanofibers, which are removed to generate hollow conductive polymer nanotubes.<sup>15</sup> In these studies, the growth of nanotubes on a template can be explained by the mechanism based on the interaction, such as solvophobic and electrostatic, between conductive polymer and a template, which was proposed by the Martin group.<sup>4b</sup> When considering only the described mechanism, however, it is difficult to explain the growth of partially filled nanotubes that are frequently observed in electrochemical template synthesis.<sup>10</sup> In our previous papers, we have given qualitative explanations for the formation of the partially filled PEDOT nanotubes by mentioning three deterministic experimental parameters: monomer concentration (concentration-gradient diffusional flux in pores), applied potential (electrochemical reaction rate), and base electrode shape at the bottom of the template pore.<sup>10</sup>

Here, we describe detailed electrochemical synthetic mechanisms and quantitative structural characterizations of various conductive polymer nanotubes in a porous alumina membrane. As a function of monomer concentration and potential, electropolymerization leads either to solid nanowires or to nanotubes, and it is the purpose of these investigations to uncover the detailed mechanism underlying this morphological transition between nanowire and nanotube. By using PEDOT as a model compound, we have systematically investigated the effects of various experimental parameters, potential, monomer concentra-

tion, base electrode shape, electrolyte concentration, and temperature, on the nanotubular structures in the pores of the template: it is the extent to which a conductive polymer nanostructure is solid or hollow that is the issue of interest, and it is the extent of nanotube filling that can be controlled using the synthesis parameters. This mechanism was applied to the synthesis of PEDOT nanotubes in the template with smaller pore diameter and other conductive polymer nanotubes such as polypyrrole and poly(3-hexylthiophene) (P3HT).

## Experimental Section

3,4-Ethylenedioxythiophene (EDOT) and 3-hexylthiophene (3HT) were obtained from Aldrich (Milwaukee, WI). Pyrrole was purchased from TCI (Portland, OR). Lithium perchlorate and acetonitrile were obtained from Acros (Morris Plains, NJ) and Fisher Scientific (Fair Lawn, NJ), respectively. Gold electroplating solution (Orotemp 24) was purchased from Technic (Cranston, RI). Deionized water (ca. 18 M $\Omega$ /cm resistivity) was obtained by using a Milli-Q water purification system from Millipore (Dubuque, IA). Alumina membranes, with a pore diameter of 200 nm and thickness of 60  $\mu$ m, are commercially available from Whatman (Clifton, NJ). Polycarbonate membrane (220 nm in diameter) was purchased from GE Osmonics (Minnetonka, MN).

Electropolymerization of EDOT was performed potentiostatically at various potentials from 1.0 to 1.8 V versus Ag/AgCl by using Pt foil (99.9%, Alfa Aesar, Ward Hill, MA) as a counter electrode in various concentrations of EDOT from 10 to 500 mM in acetonitrile solution. Electrolyte solution was 0.1 M LiClO<sub>4</sub> in an acetonitrile solution, and reaction temperature was 25  $^{\circ}$ C, if not specified otherwise. Polypyrrole was also synthesized potentiostatically in an aqueous solution. For a working electrode, one side of an alumina membrane was coated with a thin layer of gold (ca. 300 nm thick) by using an ATC 1800 3-target S-gun sputtering system (AJA international, North Scituate, MA). During this process, the sputtered gold was introduced into the pores of the membrane and forms annular electrodes at the bottom of pores. This bottom side, acting as a working electrode, was connected to a potentiostat (660A CH instruments, Austin, TX). To make flat-top electrodes in the pores, gold was deposited at a constant potential of  $-0.9$  V for 500 s by using the commercially available gold plating solution (Orotemp 24).

An alumina template with a pore diameter (ca. 80 nm) was fabricated by using a two-step anodization process.<sup>16</sup> The briefs of this process are as follows. An electropolished aluminum foil (99.99%, Alfa Aesar) was anodized at 40 V and 10  $^{\circ}$ C by using 0.3 M oxalic acid as an electrolyte. This generated an alumina layer with irregular pores. For better pore structures, this porous alumina layer was removed by using an aqueous mixture of phosphoric acid (6 wt %) and chromic acid (1.8 wt %), which exposed the barrier layer with a well-defined pre-pattern. The second anodization was performed as in the first anodization to generate well-defined pores until a desired thickness (ca. 100  $\mu$ m) was reached. After the residual aluminum was dissolved using a saturated mercury chloride solution, the removal of the alumina barrier layer and pore-widening were performed by using phosphoric acid (5 wt %) at 30  $^{\circ}$ C.

The PEDOT, polypyrrole, and P3HT nanostructures were investigated by using a field-emission scanning electron microscope (SEM; Hitachi S-4700, operated at an acceleration voltage of 5 keV) and transmission electron microscope (TEM; Zeiss EM10CA, operated at 80 keV). The sampling methods for SEM and TEM analysis were described in detail previously.<sup>1</sup> Briefly, the gold-coated side of a small piece of an alumina template was tightly attached onto an SEM specimen holder by using a carbon tape. The template was dissolved to expose the nanomaterials by using phosphoric acid (25 wt %). After being rinsed with deionized water repeatedly, the sample was dried in

- (11) (a) Szklarczyk, M.; Strawski, M.; Donten, M. L.; Donten, M. *Electrochem. Commun.* **2004**, *6*, 880–886. (b) Duvail, J. L.; Retho, P.; Garreau, S.; Louarn, G.; Godon, C.; Demoustier-Champagne, S. *Synth. Met.* **2002**, *131*, 123–128. (c) Kim, B. H.; Park, D. H.; Joo, J.; Yu, S. G.; Lee, S. H. *Synth. Met.* **2005**, *150*, 279–284.
- (12) (a) Bognitzki, M.; Hou, H.; Ishaque, M.; Frese, T.; Hellwig, M.; Schwarte, C.; Schaper, A.; Wendorff, J. H.; Greiner, A. *Adv. Mater.* **2000**, *12*, 637–640. (b) Jang, J.; Yoon, H. *Chem. Commun.* **2003**, 720–721. (c) Jang, J.; Yoon, H. *Adv. Mater.* **2003**, *15*, 2088–2091. (d) Parthasarathy, R. V.; Martin, C. R. *Chem. Mater.* **1994**, *6*, 1627–1632.
- (13) Martin, C. R. *Acc. Chem. Res.* **1995**, *28*, 61–68.
- (14) (a) Zhang, Z.; Wei, Z.; Wan, M. *Macromolecules* **2002**, *35*, 5937–5942. (b) Shen, Y.; Wan, M. *J. Polym. Sci., Part A: Polym. Chem.* **1999**, *37*, 1443–1449.
- (15) (a) Dong, H.; Prasad, S.; Nyame, V.; Jones, W. E., Jr. *Chem. Mater.* **2004**, *16*, 371–373. (b) Abidjan, M. R.; Kim, D.-H.; Martin, D. C. *Adv. Mater.* **2006**, *18*, 405–409.

- (16) Masuda, H.; Satoh, M. *Jpn. J. Appl. Phys., Part 2* **1996**, *35*, L126–L129.

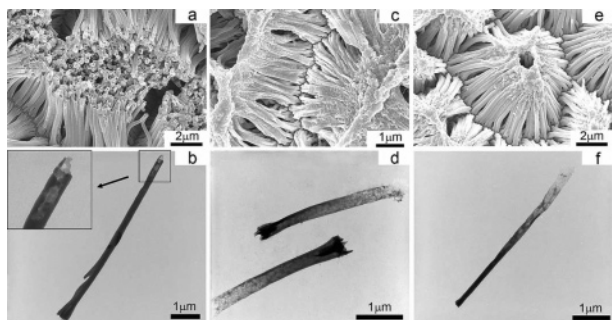


**Figure 1.** SEM and TEM images of PEDOT nanostructures synthesized potentiostatically (a,b) in 50 mM EDOT at 1.6 V, (c,d) in 50 mM EDOT at 1.2 V, and (e,f) in 25 mM EDOT at 1.5 V for 100 s. The upper (a, c, and e) and lower (b, d, and f) images were taken by SEM and TEM, respectively.

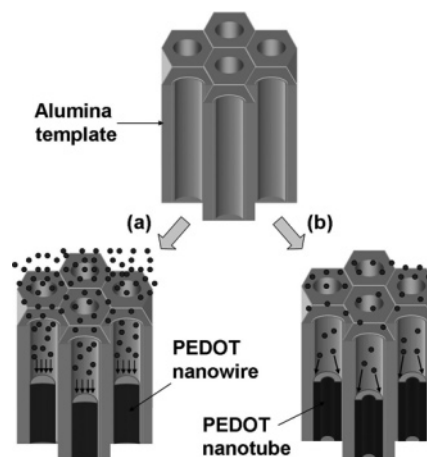
air before observation. For TEM sampling, the gold layer was removed by using an aqua regia solution after growing desired nanostructures in a gold-coated alumina template. The alumina template was dissolved by using phosphoric acid (25 wt %). The released nanomaterials were repeatedly rinsed with deionized water and ethanol. Next, 6  $\mu\text{L}$  of the nanomaterial solution was dropped and dried on a TEM grid. The error bars in this study represent the standard deviation of more than three time measurements.

## Results and Discussion

**Characterization of PEDOT Nanostructures.** It is necessary to observe and understand correctly the nanostructure of conductive polymer nanotubes to investigate their growth mechanism. The SEM images of conductive polymer nanotubes are quite different from those of metallic nanotubes because conductive polymers are not as rigid as metal. Thus, it is important to characterize correctly three different nanostructures of conductive polymer nanotubes (nanowire, partially filled nanotube, and complete nanotube) by using SEM and TEM. Here, we have chosen PEDOT as a model compound because of its well-known electropolymerization chemistry and electrochemical properties.<sup>10,17</sup> Figure 1a shows the SEM image of PEDOT nanowires that were grown in 50 mM EDOT at 1.6 V for 100 s. Because of strong surface tension at the interface between the nanowires and the solvent, PEDOT nanowires were aggregated during solvent evaporation. This phenomenon has also been observed in metallic nanostructures. PEDOT nanowire has a cylindrical shape with an open-ended tip. This shape indicates that tubular section must exist in the nanostructure. The TEM image (Figure 1b) revealed that the top 10% of the nanostructure is a hollow tube.

Figure 1c shows the SEM image of complete nanotubes that were grown in 50 mM EDOT at 1.2 V for 100 s. Unlike metallic nanotubes, it is hard to observe any open-tip structures in the SEM image of PEDOT nanotubes. Instead, the tops of the PEDOT nanotubes are highly aggregated. The bottom of the nanotubes has highly wrinkled and collapsed structures rather than smooth cylindrical structures. This implies that the nanostructures are hollow from the bottom, and the wall of nanotube is too thin to maintain its upright structure. While the wrinkled and collapsed structure in the SEM image can be a useful indicator for the formation of tubular structure, TEM studies are essential to observe and characterize the hollow structure of the nanotube such as wall thickness, inner and outer

**Scheme 1.** Growth Mechanism of PEDOT Nanostructures Based on Diffusion and Reaction Kinetics<sup>a</sup>



<sup>a</sup> The lower schemes represent the electropolymerization of EDOT (a) for slow reaction rate and sufficient monomer supply and (b) for fast reaction rate and insufficient monomer supply. The small black balls represent EDOT monomers.

diameters, and length. The TEM image in Figure 1d strongly supports that PEDOT nanostructures are completely hollow tubes with very thin wall thickness (less than 10 nm). The outer diameter of nanotubes (ca. 300 nm) is much larger than the pore diameter of the alumina template (ca. 200 nm). This indicates that the cylindrical structure of the individual nanotube became flat during the TEM sampling process due to the surface tension because the tube wall was too thin to maintain the cylindrical structure.

On the basis of the above analyses, the SEM image of partially filled nanotubes can be considered as a combination of a nanotube and a nanowire. Figure 1e illustrates the SEM image of partially filled PEDOT nanotubes grown in 25 mM EDOT at 1.5 V for 100 s. As expected, the bottom of the nanostructures resembles a nanowire, while its top resembles a nanotube. The TEM image (Figure 1f) demonstrates that 40% of the nanostructure is a nanowire. It also shows how the outer diameter of the tubular section increases toward the top of the nanotube because its tubular wall is very thin and can collapse easily.

**Effects of Applied Potential and Monomer Concentration on PEDOT Nanostructures.** The growth rate and rigidity of nanostructures in electrochemical template synthesis are determined by the applied reaction potential and monomer concentration. Thus, the growth mechanism of conductive polymer nanotubes is also influenced by these variables. Previously, we proposed a growth mechanism of PEDOT nanotubes, which considers the effects of potential and concentration on nanostructures in two extreme cases (Scheme 1).<sup>10</sup> One is the case for slow reaction rate and sufficient monomer supply. Nanowires are formed in this condition because monomers in bulk solution have enough time to diffuse into and fill the pores. The other is for fast reaction rate and insufficient monomer supply. This results in nanotubes because the monomers diffused from bulk solution are deposited along the pore wall because of the interaction of polymer and wall surface. On the basis of this mechanism, we could successfully synthesize various PEDOT nanostructures in the pores of the alumina membrane with sputtered Au layer on one side. The tubular portion of the nanotube structure increased as we increased the applied

(17) Groenendaal, L. B.; Zotti, G.; Aubert, P.-H.; Waybright, S. M.; Reynolds, J. R. *Adv. Mater.* **2003**, *15*, 855–879.

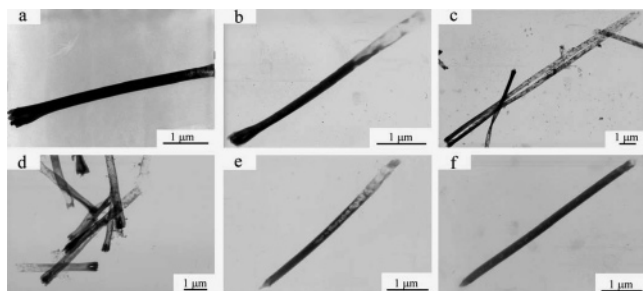


**Figure 2.** TEM images of PEDOT nanostructures in various conditions at a fixed electropolymerization time of 100 s: (a) 1.4 V, (b) 1.5 V, and (c) 1.8 V in 25 mM EDOT; (d) 1.2 V, (e) 1.3 V, and (f) 1.4 V in 50 mM EDOT.

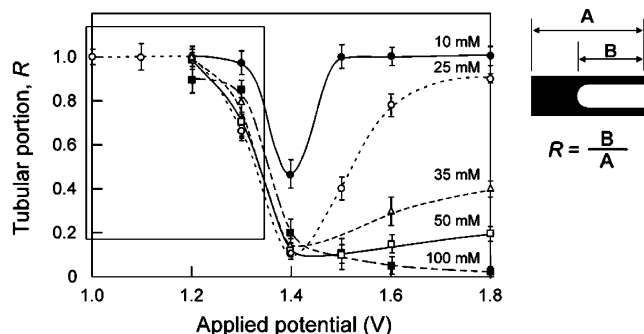


**Figure 3.** Plots of tubular portion for PEDOT nanotubes versus applied potential. Electrochemical polymerization was performed potentiostatically with the fixed polymerization time of 100 s. The tubular portion,  $R$ , is defined as the length of the tubular section divided by the total length. The data were obtained from the corresponding TEM images. The lines were added to help guide the eyes.

potential from 1.4 to 1.8 V in a fixed concentration of 25 mM EDOT (Figure 2a–c), while the tubular portion decreased as we expected by increasing the monomer concentration from 10 to 100 mM at a fixed potential of 1.6 V (data not shown here).

When we lowered the applied potential further to 1.2 V expecting to have more solid nanowires, however, we observed an interesting phenomenon (Figure 2d–f). The tubular portion in the nanotube increased again when the potential was decreased from 1.4 to 1.2 V (50 mM EDOT). This phenomenon cannot be explained by using our current mechanism.

To figure out this phenomenon, we changed the applied potential and monomer concentration systematically while fixing the electropolymerization time at 100 s. The resulting nanostructures were analyzed by using SEM and TEM and are summarized in Figure 3 by plotting the tubular portion,  $R$ , versus applied potential.  $R$  is defined as the length of tubular section divided by total length.  $R$  is then 1 for a complete nanotube and 0 for a solid nanowire. The fixed reaction time of 100 s gives a proper experimental condition that enables us to observe the electrochemical growth of PEDOT nanostructures from complete nanotube to nanowire shapes. At long enough reaction time, all PEDOT nanostructures become partially filled nanotubes and eventually solid nanowires.

At first glance, the potential dependence of PEDOT nanostructure looks complicated. Dividing the curve into two regions from 1.4 V, however, may be helpful in understanding the potential dependence of nanostructures. The tubular portion increases along with the applied potential at potentials higher than 1.4 V. This region can be well explained by using our previous mechanism based on the diffusion-limited reaction.<sup>10a</sup>

At low monomer concentration and high electropolymerization potential (e.g., 10 mM EDOT, 1.8 V), we observed that the reaction current was continuously decaying with the increase of time. The reason lies on the limited supply of monomers by diffusion. At high monomer concentration and middle-ranged electropolymerization potential (e.g., 100 mM EDOT, 1.4 V), the reaction current reached a plateau value instantly due to sufficient supply of monomers by diffusion. All of these imply that the electropolymerization of EDOT is a reaction that highly depends on diffusion.<sup>18</sup> The polymerization reaction at high potentials proceeded for the monomer consumption to exceed the monomer supply. Polymers would grow preferentially along the pore wall to form nanotubes because of the interaction of polymer and wall surface. As the potential increased, more porous, thinner, and longer nanotubes were obtained because of fast polymer growth (see the Supporting Information). At low oxidation potentials that are lower than 1.4 V, however, the growth of PEDOT nanotubes deviates from our expectation significantly. The tubular portion of the nanostructure increases even though the monomer concentration increases. Furthermore, nanotubular structures are favored nearly independent of monomer concentration at 1.2 V. These phenomena cannot be explained by using our previous mechanism based upon the diffusion and reaction kinetics.<sup>10a</sup> This implies that another mechanism is operating at low potentials, which will be discussed later.

At potentials higher than 1.4 V, monomer concentration is also an important variable to determine the PEDOT nanostructures as shown in Figure 3. It is expected that hollow nanotubes can be grown instead of solid nanowires when the polymerization reaction rate is fast enough to consume all of the monomers diffused from the bulk solution. Decreasing monomer concentration is an alternative way to achieve faster monomer consumption than monomer supply. An approximate calculation, based upon the density of PEDOT ( $\rho = 1.64 \text{ g/cm}^3$ ) obtained by X-ray diffraction,<sup>19</sup> shows that  $1.3 \times 10^{10}$  monomers (ca. 10 M EDOT in concentration) are required to fill a pore (ca.  $2 \times 10^{-12} \text{ cm}^3$  in volume). Thus, fast diffusional supply of monomers is required for the synthesis of solid nanowires in all of the conditions of current study. Because of relatively slow reaction rates, however, we could obtain full nanowires around 100 mM EDOT. Another way to increase the diffusional flux of monomers is to stir the solution or to apply a pulsed potential. This facilitated the monomer diffusion into the membrane pores, and nanowires could even be obtained in low concentrations and high voltages such as 25 mM EDOT and 1.6 V.

**Growth Mechanism of Nanotubes at Low Oxidative Overpotentials.** The base electrode shape is a deterministic factor in nanotube growth at low oxidative potentials below 1.4 V. Usually, the sputtered gold is introduced into the pores of the alumina membrane and forms annular electrode at the bottom of the pores (Figure 4a). The nanotube growth at low overpotentials may be attributed to this annular shape of gold electrode at the bottom of the pore. The oxidation of EDOT starts around 1.2 V to form PEDOT.<sup>17</sup> At this onset oxidation potential, the electrochemically active sites are critical in polymerization and dominate on top of the annular Au electrode in each pore. This

(18) Bard, A. J.; Faulkner, L. R. *Electrochemical Methods: Fundamentals and Applications*; John Wiley & Sons: New York, 1980; p 142.

(19) Aasmundtveit, K. E.; Samuelsen, E. J.; Pettersson, L. A. A.; Inganäs, O.; Johansson, T.; Feidenhans, R. *Synth. Met.* **1999**, *101*, 561–564.

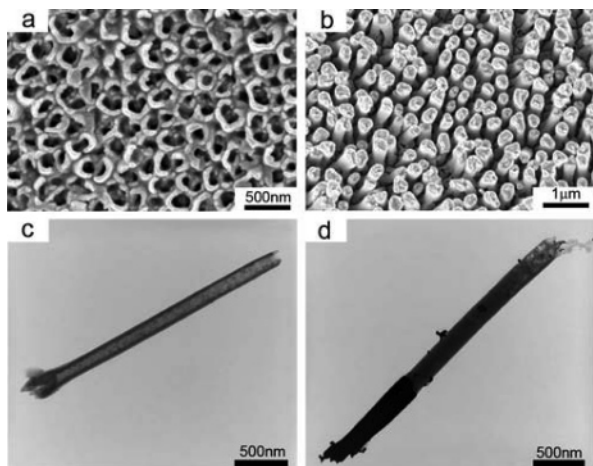


**Figure 4.** SEM images of (a) annular base electrodes (Au-sputtering only) and (b) flat-top base electrodes (Au sputtering and electrodeposition) and TEM images of PEDOT nanostructures grown at 1.2 V for 100 s (c) in 500 mM EDOT on the annular electrodes and (d) in 10 mM EDOT on the flat-top base electrodes.

high-curvature surface (sharp end) on the top of the annular Au electrode has high charge density or electric field and is electrochemically more active relative to the smooth surface. This phenomenon is called the “tip” effect.<sup>20</sup> Thus, EDOT polymerization is expected to preferentially occur on the top of the base electrode rather than on the wall surface of the base electrode.

To prove this hypothesis, we made flat-top base electrodes by further depositing gold electrochemically on the annular electrode. Figure 4b shows the SEM image of electrodeposited flat-top electrodes after removing the alumina template. The annular or sharp edge structure was eliminated via this process, and the top surface of the base electrodes was well leveled off. Next, we synthesized PEDOT on the flat top of these electrodes. In TEM sampling process, we did not dissolve the base gold electrodes so PEDOT nanostructures could be clearly differentiated from the base gold electrode in TEM images. As shown in Figure 4d, almost filled nanotube (nanowire) was fabricated even at 1.2 V. Indeed, while we could not make nanotubular structures at low oxidation potentials on the flat-top electrodes, we could synthesize nice nanotubular structures even at a very high monomer concentration (0.5 M EDOT) on the annular electrodes (Figure 4c). These results support well the hypothesis that the top surface of annular Au electrode is electrochemically more active on which to grow the nanotubular structure of PEDOT.

In the case of using the flat-top electrodes, the first mechanism regarding diffusion of monomer and polymerization reaction kinetics (applied potential) may only exist because the flat-top electrode does not have any preferential electrochemically active sites. Therefore, it is important to know if the first mechanism still works on the flat-top electrode. If it works, we will obtain a higher tubular portion ( $R$ ) in nanotubular structures as the reaction potential is increased. The tubular portion was plotted versus applied potential (Figure 5). PEDOT was synthesized by changing applied potential from 1.2 to 1.8 V at a fixed electropolymerization time of 100 s in 10 mM EDOT. Figure 5 shows exactly what we expected. The tubular portion increased

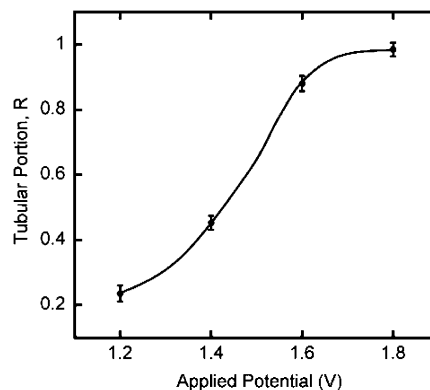


**Figure 5.** Plot of tubular portion versus applied potential for PEDOT nanostructures grown on the flat-top electrodes in the pores of alumina membrane (10 mM EDOT, 100 s in polymerization time).

as the reaction potential was increased. We have also observed the decrease of tubular portion in nanotubular structure as we increased the monomer concentration. These results strongly support that we can still use the first mechanism to control the structure of nanotube on the flat-top electrode in the template pores.

**Influences of Electrolyte Concentration and Temperature on PEDOT Nanostructures.** The flux of monomers and polymerization rates can be affected by the concentration of electrolyte ( $\text{LiClO}_4$ ) and temperature. Therefore, it is necessary to study their effect on PEDOT nanostructures, the variation of the characteristic curves in Figure 3, to have universal characteristic behaviors to selectively synthesize solid nanowires and hollow nanotubes of PEDOT materials. First, we investigated the  $\text{LiClO}_4$  concentration effect by analyzing PEDOT nanostructure (tubular portion,  $R$ ) synthesized with three  $\text{LiClO}_4$  concentrations of 0.01, 0.1, and 1 M and at three selective potentials of 1.2, 1.4, and 1.8 V. We chose the 25 mM EDOT as a model monomer concentration because PEDOT nanostructures showed the dramatic change over the applied potential in this concentration. Tubular portion was plotted as a function of applied potentials in Figure 6a at the  $\text{LiClO}_4$  concentrations of 0.01, 0.1, and 1 M. The  $R$  values at the given potential were less sensitive to the change of electrolyte concentration. However, the length of nanotubes increased dramatically as the  $\text{LiClO}_4$  concentration was increased (data not shown here). For example, the lengths of nanotubes synthesized at 1.4 V with 0.01, 0.1, and 1 M  $\text{LiClO}_4$  were 3.4, 5.2, and 6.2  $\mu\text{m}$ , respectively. These results indicate that electrolyte concentration has a greater effect on polymerization rate than on diffusion rate.<sup>21</sup> It is natural that the length of nanotubes decreases with the reduction of electrolyte concentration because the dopant,  $\text{ClO}_4^-$ , plays an important role in electropolymerization reaction rate by being incorporated into the positively charged polymer layer as a counterion during the oxidation.

Second, we studied the temperature effect by comparing the tubular portions of PEDOT nanostructures synthesized at 25 and 50  $^\circ\text{C}$  in 25 mM EDOT and 0.1 M  $\text{LiClO}_4$ . The plot of tubular portion versus applied potential (Figure 6b) shows that the nanotubes can be filled more readily at high temperature (50  $^\circ\text{C}$ ) than at low temperature (25  $^\circ\text{C}$ ). These results can be explained by the fact that the monomer flux into the pores

(20) (a) Enze, L. J. *Phys. D: Appl. Phys.* **1986**, *19*, 1–6. (b) Enze, L. J. *Phys. D: Appl. Phys.* **1987**, *20*, 1609–1615.

(21) Van den Schoor, R. C. G. M.; Van de Leur, R. H. M.; De Wit, J. H. W. *Synth. Met.* **1999**, *99*, 17–20.

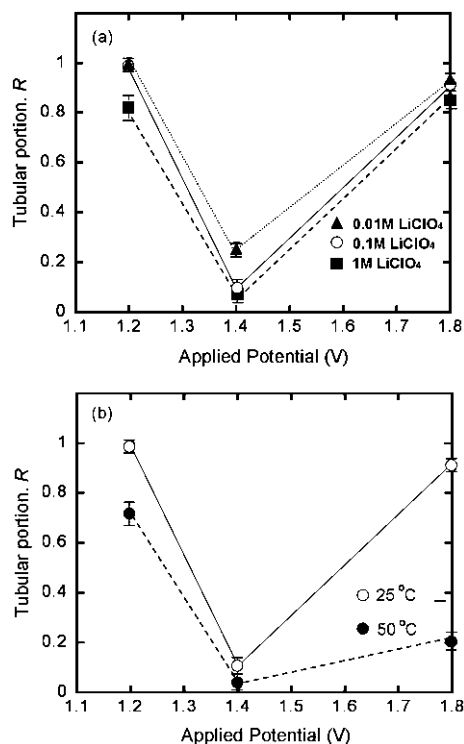


**Figure 6.** Plots of tubular portion for PEDOT nanostructures versus applied potentials. Electropolymerizations were performed at 25 °C with the LiClO<sub>4</sub> concentrations of 0.01, 0.1, and 1 M for (a), while it was done in 0.1 M LiClO<sub>4</sub> at 25 and 50 °C for (b). EDOT concentration was 25 mM in both cases.

increases significantly due to the increase of diffusion coefficient of EDOT monomer and convective mass transfer at the interface between the pores and bulk solution at the elevated temperature. Therefore, increasing temperature gives an effect similar to that of increasing monomer concentration on the PEDOT nanostructures. However, the change in nanotube lengths was less than 10% at each point and relatively insensitive to temperature change (data not shown here).

**Synthesis of PEDOT Nanotubes in the Smaller Pores.** It is more difficult to grow the nanotubular structure of PEDOT in the smaller pore, because the smaller pore may be filled faster with the PEDOT at a given electropolymerization time. However, we have successfully synthesized the PEDOT nanotubes in the smaller pore with 80 nm in diameter by using the annular Au electrode at the bottom of the pore. Figure 7a shows the SEM image of the homemade alumina template, which has a highly ordered hexagonal pattern of pores and a pore diameter of 80 nm. The bottom of the template was coated with a thin layer of gold as a working electrode. Its SEM image (Figure 7b) after removal of the template clearly shows the annular shape of Au electrode for each pore, which is helpful for the growth of nanotubular structures. The PEDOT nanotubes were successfully synthesized at 1.2 V for 100 s in 10 mM EDOT as shown in Figure 7c and d.

**Polypyrrole.** Many research groups studied the electrochemical synthesis of polypyrrole because of its potential applicabilities to sensors and electronic devices.<sup>1a,c,22</sup> However, the

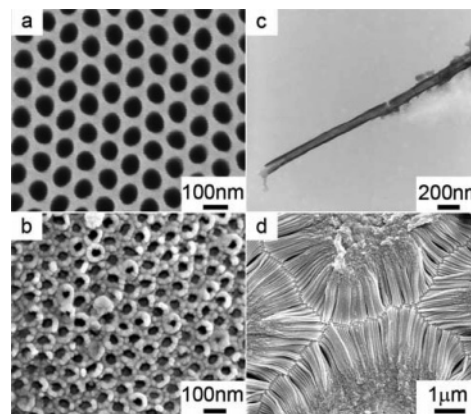


**Figure 7.** SEM images of (a) a homemade alumina template with 80-nm pores in diameter, (b) annular Au electrodes after the removal of alumina template, and (c) TEM and (d) SEM images of PEDOT nanotube synthesized at 1.2 V for 100 s in 10 mM EDOT.

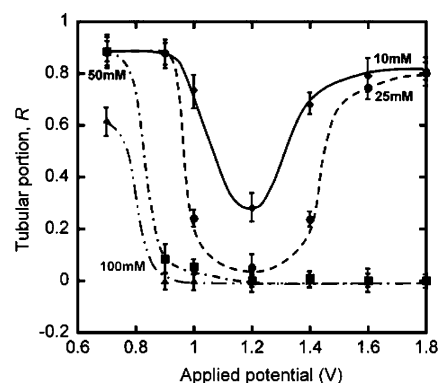


**Figure 8.** Plot of tubular portion for polypyrrole nanotubes versus applied potential.

understanding of polypyrrole nanostructures is still lacking. It is our goal to extend our mechanism study to other conductive polymers including polypyrrole.

To investigate the effect of applied potential and monomer concentration on polypyrrole nanostructures, the polymerization was performed potentiostatically in the aqueous solution of 10, 25, 50, and 100 mM pyrrole at various potentials for 100 s. The TEM data were analyzed to plot the tubular ratio versus applied potential as mentioned in the previous section. The potential dependence of polypyrrole nanostructures also has two different growth regions as shown in Figure 8. The result implies that the electrochemically active site mechanism works to grow the nanotubular structure of polypyrrole on the annular Au electrode around potentials below 0.8 V, while the diffusion and reaction kinetics mechanism works at potentials above 1.2 V to control the shape of polypyrrole nanotube. In the potential range between 0.8 and 1.2 V, the two mechanisms seem to compete with each other. The polymerization rate of pyrrole starts to increase around 0.7 V.<sup>23</sup> Thus, nanotubular structures are preferentially synthesized independent of monomer concentrations around 0.7 V. On the other hand, low monomer concentration and high potential are preferred to synthesize nanotubes at potentials higher than 1.2 V. These results strongly support that our mechanisms can be employed to the controlled electrochemical synthesis of polypyrrole nanotubes. Figure 9

(22) (a) Aquino-Binag, C. N.; Kumar, N.; Lamb, R. N.; Pigram, P. J. *Chem. Mater.* **1996**, *8*, 2579–2585. (b) Liu, X.; Ly, J.; Han, S.; Zhang, D.; Requicha, A.; Thompson, M. E.; Zhou, C. *Adv. Mater.* **2005**, *17*, 2727–2732.

(23) Hernandez, R. M.; Richter, L.; Semancik, S.; Stranick, S.; Mallouk, T. E. *Chem. Mater.* **2004**, *16*, 3431–3438.

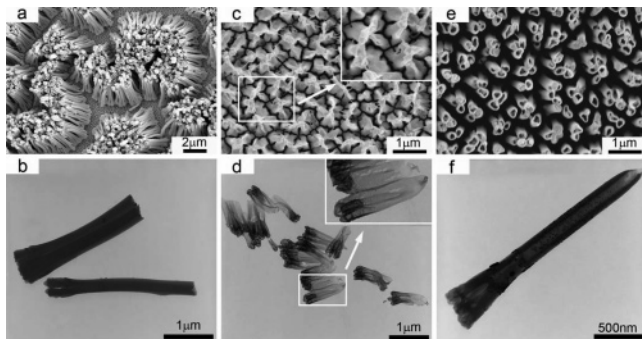


**Figure 9.** Electron micrographs of polypyrrole nanostructures synthesized potentiostatically for 100 s (a,b) in 50 mM pyrrole at 1.4 V, (c,d) in 10 mM pyrrole at 0.7 V, and (e,f) in 25 mM pyrrole at 1.8 V. The upper (a, c, and e) and lower (b, d, and f) images were taken by SEM and TEM, respectively.

shows the representative electron microscopic images of polypyrrole nanostructures synthesized at three different conditions. In addition, the P3HT nanowires and nanotubes were also synthesized electrochemically based on the same mechanisms (see the Supporting Information).

## Conclusion

We have successfully investigated two electrochemical synthetic mechanisms of conductive polymer nanotubes in a

porous alumina template using PEDOT as a model compound. The mechanism based on electrochemical active site works to grow the nanotubular structure of PEDOT on the annular Au electrode at the potentials below 1.4 V, while the mechanism based on diffusion and reaction kinetics works at the potentials above 1.4 V to control the shape of PEDOT nanotube. These mechanisms were also successfully employed to control the dimensions of other conductive polymer nanotubes such as polypyrrole and P3HT. The current systematic, quantitative study about nanotube filling as a function of various experimental parameters and the elaborated mechanism will give some insight into the controlled synthesis of conductive polymer nanotubes.

**Acknowledgment.** This work was supported by the Laboratory for Physical Sciences, National Science Foundation, under the MRSEC Grant DMR-05-20471 and the University of Maryland. We thank Tim Mangel (Laboratory for Biological Ultrastructure, University of Maryland) for assistance with SEM and TEM.

**Supporting Information Available:** Details of the control of nanotube length and rigidity; the electrochemical synthesis of P3HT nanotubes. This material is available free of charge via the Internet at <http://pubs.acs.org>.

JA068924V